Impact of biomass burning on cloud properties in the Amazon Basin

G. C. Roberts

Max Planck Institute for Chemistry; California Institute of Technology

A. Nenes and J. H. Seinfeld

California Institute of Technology

M. O. Andreae

Max Planck Institute for Chemistry

Abstract. We used a 1-D cloud parcel model to assess the impact of biomass-burning aerosol on cloud properties in the Amazon Basin and to identify the physical and chemical properties of the aerosol that influence droplet growth. Cloud condensation nuclei (CCN) measurements were performed between 0.15 and 1.5% supersaturation at ground-based sites in the states of Amazonas and Rondônia, Brazil, during several field campaigns in 1998 and 1999 as part of the Large Scale Biosphere-Atmosphere Experiment in Amazonia (LBA). CCN concentrations measured during the wet season were low and resembled concentrations more typical of marine conditions than most continental sites. During the dry season, smoke aerosol from biomass burning dramatically increased CCN concentrations. The modification of cloud properties, such as cloud droplet effective radius and maximum supersaturation, is most sensitive at low CCN concentrations. Hence, we could expect larger inter-annual variation of cloud properties during the wet season that the dry season
We found that differences between CCN spectra from forested and deforested regions during the wet season are modest, and result in modifications of cloud properties that are small compared to those between wet and dry seasons. Our study suggests that the differences in surface albedo, rather than cloud albedo, between forested and deforested regions may dominate the impact of deforestation on the hydrological cycle and convective activity during the wet season. During the dry season, on the other hand, cloud droplet concentrations may increase by up to seven times which leads to a model-predicted decrease in cloud effective radius by a factor of two. This could imply a maximum indirect radiative forcing due to aerosol as high as ca. -27 W m^{-2} for a non-absorbing cloud. Light-absorbing substances in smoke darken the Amazonian clouds and reduce the net radiative forcing, and a comparison of the AVHRR analysis and our modeling studies suggests that absorption of sunlight due to smoke aerosol may compensate for about half of the maximum aerosol effect.
Sensitivity tests show that complete characterization of the aerosol is necessary when kinetic growth limitations become important. Subtle differences in the chemical and physical make-up are shown to be particularly influential in the activation and growth behavior of the aerosol. Knowledge of the CCN spectrum alone is not sufficient to fully capture the climatic influence of biomass burning.

1. Introduction

Biomass burning in the Amazon Basin [*Setzer and Pereira*, 1991] generates a smoke pall of variable density across millions of square kilometers during the dry season between June and December. A complex interaction among water vapor, cloud condensation nuclei (CCN) abundance, light absorption by "black carbon", and atmospheric stability affects the strength of convection and subsequent cloud development and cloud albedo. Measurements during the dry season reveal a stable spatial distribution of water vapor in contrast to the variability of aerosol concentrations [*Kaufman et al.*, 1992]. Hence, the cloud optical properties in the Amazon dry season may be less dependent on variations of the meteorological conditions than those of CCN. Smoke aerosol dramatically increases CCN concentrations, which could lend to increased cloud droplet stability and cloud lifetime [*Albrecht*, 1989]. The influence of smoke on rain formation was also shown during the Tropical Rainfall Measuring Mission (TRMM) taken near Kalimantan, where a distinct difference in cloud structure and radar reflectance was seen between clouds influenced by biomass burning and those in cleaner areas. Clouds in cleaner areas had warmer and larger drops than the non-precipitating clouds affected by smoke [*Rosenfeld*, 1999].

AVHRR (Advanced Very High Resolution Radiometer) analysis during the 1987 biomass burning season in the Amazon Basin also demonstrated the direct influence of smoke on cloud properties [*Kaufman and Fraser*, 1997]. Their study showed that smoke particles reduced droplet size from 14 to 9 μm and increased the reflectance of thin to moderately thick clouds from 0.35 to 0.45. In a previous study, remote sensing of smoke and cloud properties over the Amazon Basin showed a similar decrease in effective droplet radius and a decrease in reflectance from 0.71 to 0.68 due to the absorption of sunlight by biomass-burning aerosol [*Kaufman and Nakajima*, 1993]. However, only the bright clouds that are strongly affected by biomass-burning aerosol were used in the analysis, thus obscuring the effects of CCN on cloud reflectance.

Effective cloud droplet radii have decreased by 10 to 15% in the Amazon Basin from 1985 to 1995 (AVHRR analysis by T. Nakajima, personal communication, 2000). The reduction in cloud droplet radii has been more significant during the wet season (i.e., 13.6 to 11.8 μm) compared to the dry season (i.e., 9.7 to 9.0 μm) and may be related to the rapid demographic and land-use changes in the Amazon Basin during this period. Recent studies of radar and satellite observations in the Amazon Basin have shed light on the roles of updraft and aerosol in influencing the maritime or continental behavior of clouds [*Williams*, 2002]; extreme cases were identified in which either the updraft or aerosol dominate cloud development. The aerosol is important because of its effect on droplet size and hence collision/coalescence processes. The updraft velocity is crucial because of its effect on the time available for coalescence, its ability to raise particles above the freezing level and subsequent generation of ice nuclei.

The motivation of our work is to assess the potential impact of human development in the Amazon Basin, and in particular the effect of smoke aerosol on cloud properties. Measured wet-season CCN spectra differ dramatically from dry-season spectra due to the presence of biomass-burning aerosol. In the following sections, we explore cloud droplet formation for measured CCN spectra in the Amazon Basin using a 1-D cloud parcel model with detailed aerosol microphysics. This model incorporates water vapor growth kinetics and is discussed in detail by *Nenes et al.* [2001b]. Measurement uncertainties and approximations preclude an exact representation of the aerosol population; hence, we examine the dependence of cloud properties on the chemical and physical make-up of the aerosol in the form of a sensitivity analysis. The model calculations are should not be used for prognostic purposes, but to diagnose the sensitivity of droplet nucleation to changes in the CCN population. Expressing changes in droplet concentration in terms of changes in effective radius and albedo, give a physically-based measure of the importance of an e.g. 1% increase in droplet number.

2. Experimental Description

2.1. Site Description

The measurements were performed as part of the Large Scale Biosphere-Atmosphere Experiment in Amazônia (LBA) in 1998 and 1999, during the wet and dry seasons. LBA is an international research initiative designed to study the interactions between Amazônia and the earth system. The Cooperative LBA Airborne Regional Experiment (LBA-CLAIRE) took place during the wet season from 28 March to 15 April 1998, and included measurements at a ground site (Balbina, 1^o 55.5' S, 59^o 24.8' W; 160 m above sea level) located 125 km northeast of Manaus, in the state of Amazonas, Brazil. Backward airmass trajectory calculations indicate that our site was not affected by anthropogenic sources, as surface air masses originated from the northeast to east;

hence had traveled a thousand kilometers over the most remote regions of the Amazon rain forest for almost a week before being sampled. Inlets for all instruments were located 6 m above the ground, via individual sampling lines that extended 2 m above the roof of the laboratory.

In 1999, the European Studies on Trace gases and Atmospheric Chemistry experiment (LBA-EUSTACH) extended operations to include wet- and dry-season measurements [*Andreae*, 2002]. Forest and pasture sites near Ji-Paraná in the state of Rondônia were selected to characterize the influence of human settlement and deforestation in the Amazon Basin. The wet-season measurements continued into the beginning of the burning season, when fires began in the neighboring state of Mato Grosso. The dry-season experiment occurred from 15 September to 1 November 1999, encompassing the period from the peak of fire activity (beginning to middle of September) to the onset of the wet season (end of October). The forest site was located in the Jarú Biological Reserve (10^o 05.07' S, 61^o 55.92'; 130 m above sea level) about 90 km north of Ji-Paraná along the Machado River. Measurements took place at 50 m height on a meteorological tower to characterize the composition of the mixed boundary layer. The surrounding forest canopy is approximately 30 m high. During the wet season, anthropogenic contributions to the ambient aerosol were minimal, since the prevailing wind direction was mostly from forested regions to the east. The pasture site was located on the Fazenda Nossa Senhora (10^o 45.78' S, 62^o 21.45' W; 270 m above sea level) about 50 km to the east of Ji-Paraná. Sampling for each instrument took place 5 m above the ground via individual inlets that were extended 1.5 m above the roof of the laboratory. The deforested region extends for at least 60 km surrounding the pasture site. As a consequence, anthropogenic contributions from local traffic, charcoal factories, and nearby cities (i.e., Ouro Preto d'Oueste and Ji-Paraná) influenced aerosol properties at the site, representing conditions that are fairly typical for deforested parts of the Amazon.

2.2. Instrumentation

We measured CCN concentrations, N_{CCN}, at supersaturations, S_v, between 0.15 and 1.5% using a static thermal-gradient chamber. The operation of the instrument is similar to the chamber described by *Lala and Jiusto* [1977]. Instead of the original light-scattering design, our CCN counter was fitted with a photodiode laser and digital camera to measure droplet concentrations. A detailed description of the CCN counter and calibration procedure is found in *Roberts* [2001]. A 670 nm wavelength photodiode laser illuminates the activated droplets while the digital camera, normal to the laser beam, registers images every second during the supersaturation cycle. The CCN concentration at a particular supersaturation is determined during post processing. Imaging software automatically determines the number of activated CCN in each image. The CCN concentration is calculated based on the image with the highest number of particles and on the calibrated illuminated volume. The calibration procedure involved generating a quasi-monodisperse aerosol of a known concentration and counting the number of activated droplets in the digital image. An error analysis for calibration measurements indicates that for typical aerosol spectra, the overall measurement error in number concentrations is approximately $\pm 15\%$ at 1.5% S_v and $\pm 30\%$ at 0.15% S_v. These uncertainties are in agreement with theoretical predictions by *Nenes et al.* [2001a].

CCN number concentrations were determined every 25 s at a series of supersaturations between 0.15 and 1.5 % S_v, yielding a complete CCN spectrum in six to seven minutes. A CCN cycle begins with a seven-second flush at 3 liters min^{-1} to remove the previous sample and draw in air for a new sample. The instrument's inlet valve closes and isolates the chamber, which allows the supersaturation profile to develop between two horizontal parallel wetted plates. The CCN counter operates at a desired supersaturation by controlling the temperature difference between the wetted plates. The diameter of the chamber is 100 mm and the top and bottom plates are separated by 10 mm. These dimensions allow for air in the chamber to reach an equilibrium supersaturation profile in several seconds. Whatman filter papers on the top and bottom plates are kept wetted by an external capillary system. The top plate temperature is allowed to float with the ambient temperature, which ranged from 20 to 35^oC, and the bottom plate is cooled as necessary to achieve the prescribed supersaturation. Temperature fluctuations during measurements are usually within 0.1^oC, so the supersaturation is constant within $\pm 0.05\%$ S_v. Activated CCN particles quickly grow to several micrometers in diameter and gravitationally settle out of the chamber.

3. Model Description

3.1. Cloud Parcel Model

A cloud parcel model [*Pruppacher and Klett*, 1997; *Seinfeld and Pandis*, 1998] is the simplest tool that

can be used to simulate the evolution of droplet distributions throughout a non-precipitating cloud column. It also predicts the maximum influence of aerosol on cloud properties because it focuses on the early stages of cloud formation, where droplets are produced through diffusional growth. The cloud parcel model used for this study includes explicit aerosol microphysics [*Nenes et al.*, 2001b] and can account for the presence of slightly soluble and surfactant substances. For this study, the parcel is assumed to be adiabatic.

3.2. Cloud Optical Properties

Cloud albedo, R_c, is calculated based on the two-stream approximation of a non-absorbing, horizontally homogeneous cloud [*Lacis and Hansen*, 1974] (e.g., non-precipitating stratocumulus clouds),

$$R_c(z) = \frac{\tau}{7.7 + \tau}$$

where τ is the cloud optical depth,

$$\tau = \int_0^H \frac{3\rho_a w_L(z)}{2\rho_w r_{eff}(z)} dz$$

and $w_L(z)$ is the liquid water mixing ratio (kg water kg^{-1} air) profile along the cloud column. ρ_w is the water density (kg m^{-3}), ρ_a is the air density (kg m^{-3}), and $r_{eff}(z)$(m) is the cloud droplet distribution effective radius. The difference in cloud albedo at height z is used to assess modifications in cloud properties between the different simulations.

The cloud droplet effective radius was computed by

$$r_{eff} = \frac{\int_0^\infty r^3 n(r) dr}{\int_0^\infty r^2 n(r) dr}$$

where $n(r)$ is the droplet size distribution. For the optical depth calculations, we use, by default, the definition of effective radius (equation 3). To assess the albedo difference between the equilibrium cloud droplet population and that computed on the basis of dynamic mass transfer of water (see sections 3.3 and 6.3), we assume a monodisperse droplet population that has a certain amount of available liquid water. For this special case, the expression for $r_{eff}(z)$ is given by

$$r_{eff}(z) = \left(\frac{3\rho_a w_L(z)}{4\pi\rho_w N_d(z)} \right)^{\frac{1}{3}}$$

where $N_d(z)$ is the droplet concentration (m^{-3}) and is equal to the number of particles that are larger than the activated particle with the smallest dry diameter. We invoke the monodispersity assumption only when assessing the extent of kinetic limitations when comparing kinetic with thermodynamic albedo. This is done because thermodynamic activation by definition does not prescribe size distribution information, only total droplet number. So, when computing optical properties, in order to avoid systematic biases, we use a consistent base, which for simplicity, is provided by using equation 4.

3.3. Kinetic Limitations

While it is often assumed that particles are always at equilibrium with the local ambient water vapor concentration, cloud droplets, however, need a finite time to grow. As a result, the assumption of equilibrium can lead to an overestimation in droplet number as a result of mass transfer limitations [*Nenes et al.*, 2001b].

The importance of kinetic growth limitations for droplet formation will be measured in terms of both droplet number and cloud albedo. For this purpose, the number concentrations of droplets, N_{eq} and N_{kn}, based on equilibrium and kinetic approaches, respectively, are required. N_{eq} is based on the assumption that particles activate instantaneously and represents the upper limit to the number of droplets that can be formed. N_{kn} is the droplet concentration from the 1-D dynamic parcel model [*Nenes et al.*, 2001b]. Based on the variation of N_{kn} and N_{eq} with cloud depth, z, one can define another useful quantity, the total droplet ratio, $\alpha(z)$,

$$\alpha(z) = \frac{N_{kn}(z)}{N_{eq}(z)}$$

which expresses the ratio of actual droplets formed to the maximum droplets attainable at a certain cloud depth. Vertical profiles of the activation ratios can provide insight regarding the importance of kinetic limitation mechanisms [*Nenes et al.*, 2001b].

4. CCN Spectra Measurements

CCN spectra measurements for all the field campaigns are summarized in Figure 1. CCN number concentrations during wet-season field campaigns were low and resulted in a spectrum typical of oceanic environments [*Roberts et al.*, 2001a]. The LBA-CLAIRE and LBA-EUSTACH experiments took place in 1998 and 1999, respectively, at sites nearly 1000 km apart; yet,

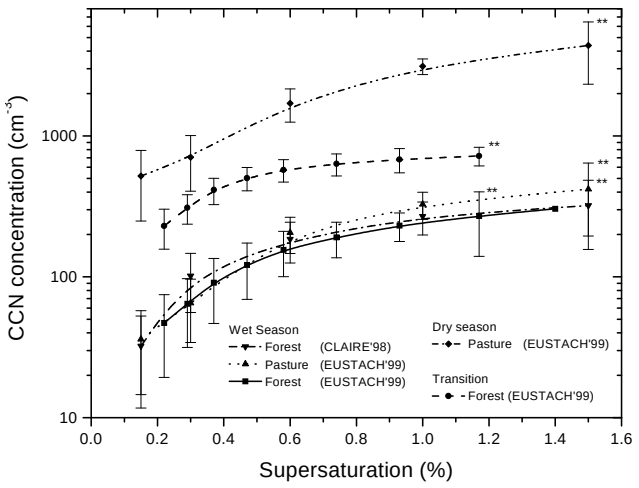

Figure 1. Summary of cumulative CCN spectra measured for wet, transition and dry seasons in the Amazon Basin. The error bars indicate one sigma variation in the CCN spectra normalized to its highest supersaturation, except for the error bars at the highest supersaturation of each spectrum. ** These error bars represent one sigma variation in the CCN number concentration for the selected sample period.

the wet-season CCN spectra were nearly identical regardless of the sampling location and the year. The uniformity of physical and chemical aerosol properties suggests a common biogenic source of the aerosol throughout the Amazon Basin. Hence, we consider the forest site wet-season CCN spectrum as representative of the natural background Amazonian CCN spectrum and as a reference to which a change in cloud properties may be compared.

The pasture site wet-season CCN spectrum was similar to that of the wet-season forest site. However, there is a slight shift to higher CCN concentrations at larger supersaturations due to local anthropogenic aerosol sources. The significance of this enhancement in the CCN spectra will be characterized in later sections and yields useful information regarding the potential changes due to human development in the Amazon Basin.

At the end of the wet season (e.g., middle of May 1999), biomass burning began in the neighboring state of Mato Grosso. Isentropic backward airmass trajectories [*NOAA-ARL*, 1997] indicate that the surface air masses originated from the east; hence had traveled several hundred kilometers over the Amazon rain forest for a couple of days before being sampled. We observed a strong diel cycle in CCN concentrations that varied by nearly a factor of two, which suggests evidence of coupling aerosol transport to the development of the boundary layer. Obvious changes to the CCN spectra were observed as the fire activity increased during the transition period. CCN concentrations increased and the shape of the spectra changed, as well. The enhanced "curvature" of the transition period CCN spectrum (Figure 1) probably occurs because of a shift to a larger median diameter of the number distribution of aged smoke aerosol [*Reid et al.*, 1998].

During the dry season, N_{CCN} were highly variable depending on the proximity of the burning and averaged about an order of magnitude higher than during the wet season. The spectra were similar to measurements at mid-latitudes near urban centers [*Hobbs et al.*, 1985; *Hudson and Frisbie*, 1991] and oil-fire plumes in Kuwait [*Hudson and Clarke*, 1992]. The sources of the biomass-burning aerosol included local fires and aged smoke that had been transported from other regions in Brazil.

5. Simulation Parameters

To investigate the relationship between the CCN spectra and the development of convective cloud formation in the boundary layer, we used 1-D parcel model. With this model, we explored the sensitivity of effective cloud radius, albedo, and maximum parcel supersaturation on physical and chemical properties of the aerosol population. Size distributions of lognormal form were used to represent the aerosol for which CCN spectra had been measured,

$$\frac{dN_i}{d\ln d_p} = \frac{N_i}{\sqrt{2\pi}\ln\sigma_{g,i}} \exp\left[\frac{-(\ln d_p - \ln d_{pg,i})^2}{2\ln^2\sigma_{g,i}}\right]$$

where N_i is the aerosol number concentration, $d_{pg,i}$ is the geometric median diameter, and $\sigma_{g,i}$ is the geometric standard deviation for mode i. We assume an aerosol distribution assumed to be composed of either one (i= 1 only) or three (i= 1,2,3) such modes, which is specified in Table 1.

Values for N (sum of N_i), d_{pg}, and σ_g that best represent the measured CCN spectra are given in Table 1. A particle's critical supersaturation, S_c, is determined for a two-component aerosol based on measured literature values for the amount of NH_4HSO_4 [*Reid et al.*, 1998; *Roberts et al.*, 2001b] and water-soluble organic compounds (WSOCs) [*Mayol-Bracero et al.*, 2002]. WSOC content was divided into neutral, mono/di- acids, and

Table 1. Size Distribution Parameters for CCN Spectra.

season	ID	number distribution			NH_4HSO_4	OC
		N, cm^{-3}	D_{pg},μm	σ_g	mass fraction	mol C liter^{-1}
Wet season	WA	458.7	0.083	1.83	0.055	0
	WB	458.7	0.083	1.83	0.0611	0
	WCST	458.7	0.083	1.83	0.035	0.01
	WMST[a]	338.8	0.072	1.541	0.055	0
		92.37	0.163	1.307	0.15	0
		19.05	0.900	1.419	0.02	0.01
Pasture site	PA	550	0.086	1.83	0.055	0
	PB	500	0.100	1.83	0.055	0
Transition	TA	770	0.150	1.706	0.055	0
	TB	830	0.140	1.738	0.055	0
Dry season	DA	5200	0.090	1.896	0.056	0
	DB	5200	0.120	1.801	0.019	0
	DC	5200	0.150	1.706	0.007	0
	DDST	5200	0.090	1.896	0.02	0.035
	DEST	6000	0.090	1.896	0.02	0.01

Each case was run at constant updraft velocities of 0.1, 0.3, 1.0 and 3.0 m s^{-1}. For all cases except WMST, the insoluble core density was 1.55 g cm^{-3}.

[a]WMST is a tri-modal distribution that also contained an insoluble core of 2.5 g cm^{-3}in the 0.900 μm mode (mass fraction = 0.13). The remainder of the mass fraction was organic carbon (OC).

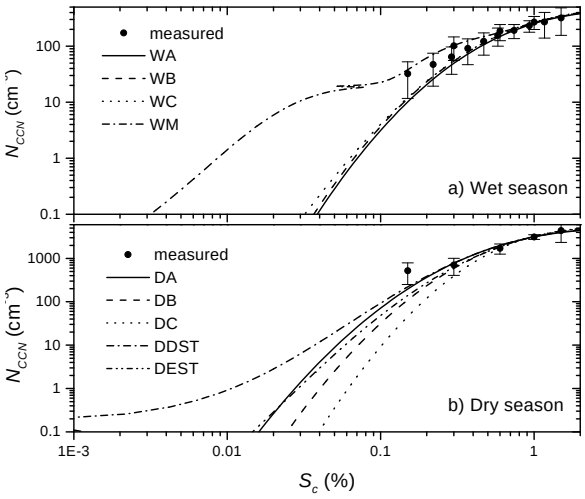

Figure 2. Modelled and measured CCN spectra for the wet and dry season. The simulations (WA, WB, etc.) are defined in Table 1.

polycarboxylic acids whose mass ratios and molecular weights are described in Table 2. Although this is not a unique representation, it is quite realistic as reflected by the recent work of *Fuzzi et al.* [2001]. WSOCs enhance CCN activity by adding soluble material and reducing the surface tension of liquid cloud droplets. *Facchini et al.* [1999] determined the relationship between dissolved WSOC concentrations and the reduction in surface tension for ambient atmospheric cloud water samples, which was applied here to estimate potential influences of surfactants on CCN spectra and subsequent cloud properties.

The properties of all the aerosol components are shown in Table 2. The size distribution and relative mass fraction of each component (Table 1) were chosen to accurately describe measured CCN spectra (Figures 1 and 2). Parameters were either measured or constrained based on previous experiments. The number distribution was first determined, and chemical composition was adjusted to yield a CCN spectrum that matched the measured spectrum. The error bars in the figures represent the resulting one-sigma variations between the simulations for a particular season.

The wet-season number distribution was directly measured during the CLAIRE experiment [*Zhou et al.*, 2002] and fitted to a single or tri-modal lognormal distribution (Table 1). By varying the chemical properties of the single mode distributions, we assessed the effect of WSOCs. A tri-modal distribution with a composition similar to the average chemical composition reported in *Roberts et al.* [2001b] serves as a "realistic" wet-season aerosol distribution. The principal difference is the addition of a large mode at 0.90 μm, which illustrates the effects of the "giant" CCN (GCCN).

Wet-season pasture site CCN spectra were nearly identical to the forest data except for a slight increase in N_{CCN} at higher supersaturations, which can be accounted for in the model by increasing N and/or d_{pg} of the wet-season number distribution. Anthropogenic inputs, such as exhaust from diesel automobiles or nearby factories, increase aerosol concentrations and may contribute to a larger median diameter in the size distribution [*Kleeman et al.*, 2000]. Two alternative number distributions were investigated for the pasture site CCN spectrum by varying d_{pg} and N of the wet-season forest size aerosol distribution (Table 1).

Number distribution measurements for the transition and dry-season spectra were not available; as a result, approximations were made based on literature values. Since both the transition and dry-season CCN spectra involved biomass smoke aerosol, d_{pg} and σ_g were constrained by a linear relationship reported by *Reid et al.* [1998],

$$\sigma_g = \lambda_1 d_{pg} + \lambda_2$$

where λ_1 =-3.16 μm^{-1}, λ_2= 2.18 and $0.09 < d_{pg} < 0.28$ μm is the maximum range allowed based on measurements during the SCAR-B (Smoke, Clouds and Radiation-Brazil experiment) [*Kaufman et al.*, 1998]. These constraints on the geometric median diameter limit the range of the geometric standard deviation to $1.3 < \sigma_g < 1.9$. Smoke particles evolve rapidly after emission, and their physical and chemical properties are related to their age. Young smoke exhibits a smaller median diameter than aged smoke and could be reflected by the difference in CCN spectra between the dry and transition periods. The more pronounced "curvature" in the transition period CCN spectra is indicative of aged, larger smoke aerosol, which was transported for several days over the rain forest.

Since a large fraction of the biomass-burning aerosol consists of water-soluble and humic-like substances [*Mayol-Bracero et al.*, 2002], solubility and surface tension effects of this aerosol may play an important role in increasing the CCN activity during the dry season. *Reid et al.* [1998] also report average sulfate composition for biomass-burning smoke aerosol to be several percent of the total aerosol mass (i.e., 1-2% for young aerosol and < 7.6% for aged aerosol). Hence, the physical and chemical properties of the dry-season aerosol were selected

Table 2. Properties of Important Components Used in Köhler Theory to Estimate CCN Activity.

Material	Density ($g\ cm^{-3}$)	Molecular weight ($g\ mol^{-1}$)	Solubility (mole $liter^{-1} H_2O$)	Van't Hoff factor
NH_4HSO_4	1.780	115.11[a]	6.55[a]	2.0
WSOC	1.55[b]	194.3[b]	0.01 (carbon)[c]	2.79
Insoluble inorganic	2.5[d]	NA	0.0	0.0
Insoluble organic	1.55[b]	NA	0.0	0.0

[a]CRC Handbook [*Lide*, 2000]

[b]Facchini (person communication); neutral compounds (18% by mass of WSOC) can be modeled as levoglucosan (162 g mol^{-1}, 1.6 g cm^{-3}, van't Hoff factor (vH) = 1); mono/di-acids (41% by mass of WSOC) can be modeled as succinic acid (118 g mol^{-1}, 1.572 g cm^{-3}, vH = 3); Poly-carboxylic acids (41% by mass of WSOC) can be modeled as fulvic acid (732 g mol^{-1}, 1.5 g cm^{-3}, vH = 5)

[c]*Facchini et al.* [1999]

[d]average crustal material [*Mason*, 1966]

based on literature values and constrained to fit the measured CCN spectra between 0.15 and 1.5% S_v. As the mode diameter or surface tension effects increase, the amount of soluble material (i.e., NH_4HSO_4) must be reduced (see Table 1) to maintain agreement between modeled and observed CCN spectra. Such chemical and physical differences in aerosol properties will affect cloud droplet growth and result in a range of cloud properties. The effect of GCCN was not studied for the biomass-burning aerosol; however, the presence of GCCN can enhance the development of precipitation in mixed-phase convective clouds in regions with high aerosol concentrations [*Yin et al.*, 2000].

The sensitivity of cloud properties was also calculated as a function of increasing aerosol number concentration using the size distributions obtained during the wet season at the forest site. The median diameter, median standard deviation, and chemical composition of simulation WA (Table 1) were kept constant, while the number concentration was varied from 10^2 to 10^4 cm^{-3}. The wet-season forest site spectrum provides a reference to assess the effects of increasing aerosol concentration on cloud properties in the Amazon Basin due to the input of anthropogenic aerosol.

6. Cloud Properties of Average Aerosol Distributions

The effects of biomass burning and the sensitivity of wet-season cloud properties are considered for the measured CCN spectra in the Amazon Basin (Figure 1).

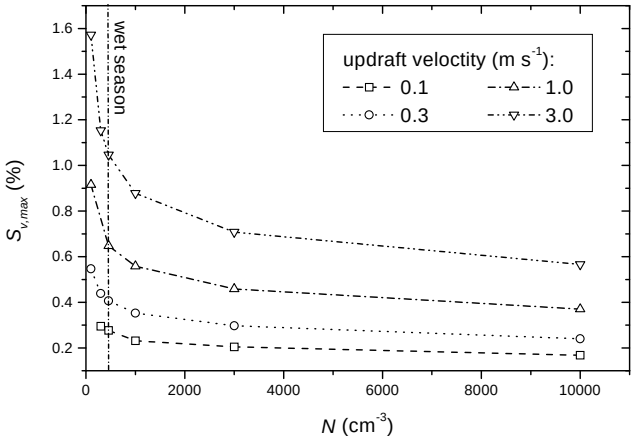

Figure 3. Cloud parcel maximum supersaturation as a function of increasing aerosol concentrations using the wet-season forest site CCN number distribution (WA). Each curve represents a different updraft velocity.

This section presents the cloud properties based on an ensemble average for each season (e.g., the mean droplet number for the dry season was based on the average droplet number of the five dry-season simulations). Error analysis reflects the inter-seasonal variance of the ensemble average for each season.

Wet-season CCN spectra allowed for maximum supersaturations that were nearly two times higher than for the dry-season spectra (Table 3). Maximum parcel supersaturation attained in the cloud increased with up-

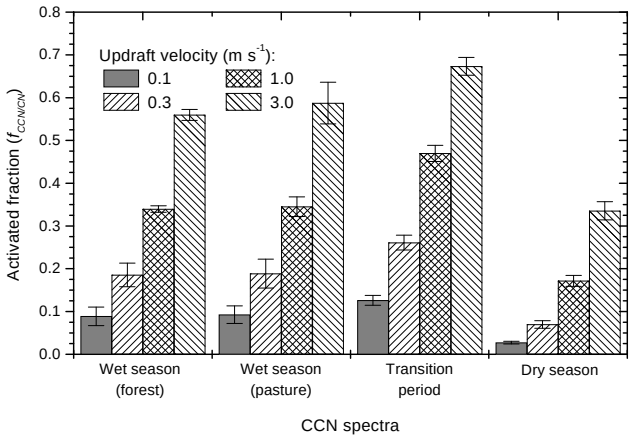

Figure 4. Fraction of aerosol that serve as CCN, $f_{CCN/CN}$, for the measured CCN spectra in the Amazon Basin. The error bars in this and the following figures represent one-sigma variations for a particular season using the simulations from Table 1.

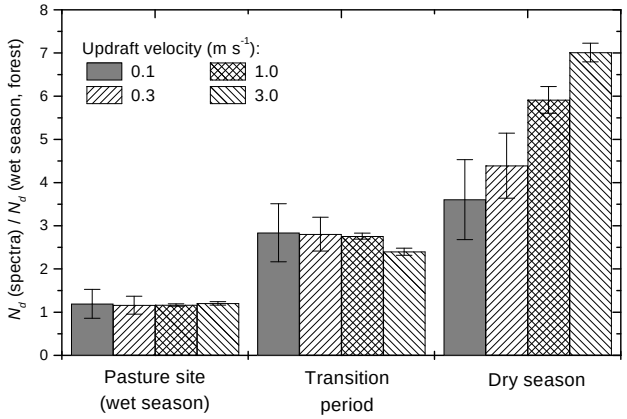

Figure 5. Ratio of cloud droplet concentration between the measured CCN spectra in the Amazon Basin and the wet season. The wet-season forest site CCN spectrum was used as a reference.

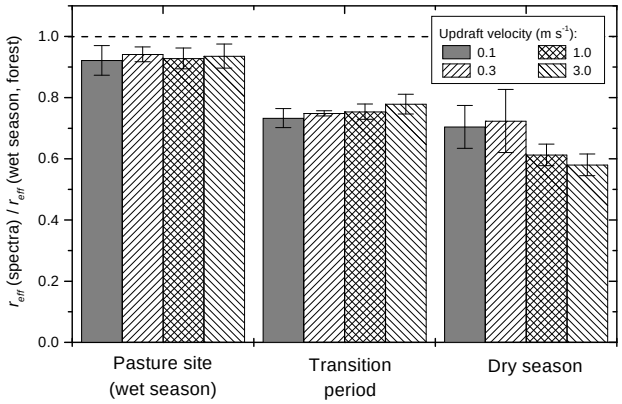

Figure 6. Ratio of effective cloud radius between the measured CCN spectra in the Amazon Basin and the wet season. The wet-season forest site CCN spectrum was used as a reference.

draft velocity due to the higher rates of adiabatic cooling and decreased with increasing N (and N_d) because of the competition for water vapor by more particles. The reduction in maximum parcel supersaturation is a nonlinear function of N_{CCN} and is most sensitive at low concentrations (Figure 3), such as those observed during the wet season.

6.1. Cloud Droplet Number

The cloud droplet number is a key parameter in regulating cloud properties. As evapotranspiration maintains a relatively uniform spatial distribution of water vapor above the forest canopy, cloud droplet number is primarily dependent on updraft velocity and the CCN spectra. The fraction of aerosol that serves as CCN, $f_{CCN/CN}$, for each of the simulated size distributions is shown in Figure 4. In spite of the lower parcel supersaturations for the transition period (Table 3), the larger mode diameter allows for higher $f_{CCN/CN}$ than during the wet season. For the dry-season spectra, on the other hand, $f_{CCN/CN}$ are less than for the wet season due to the order of magnitude increase in number concentrations and the enhanced kinetic growth effects.

The fractional increase in cloud droplet number concentration compared to the wet-season (forest) reference spectrum is shown in Figure 5. The differences in droplet concentrations between the wet-season forest and pasture sites are minimal. This similarity in droplet concentration is expected since the maximum parcel supersaturation is 0.82% (at 3.0 m s^{-1} updraft velocity; Table 3), and the CCN spectra for the forest and pasture sites are nearly identical for $S_c < 0.82\%$. The initial conditions and dynamic forcing for these simulations are the same in order to isolate the effect of the aerosol properties on clouds. Significant differences in the water vapor content and surface heating rates resulting from the different land-cover could, however, induce dramatic changes in convective activity.

Biomass burning yields up to a seven-fold increase

Table 3. Simulated Maximum Supersaturations as a Function of Updraft Velocity for Different Periods in the Amazon Basin.

Updraft vel.(m s^{-1})	Maximum supersaturation, $S_{v,max}$ (%) Wet season[a](forest)	Wet season (pasture)	Transition period	Dry season
0.1	0.270 ± 0.007	0.253 ± 0.013	0.191 ± 0.001	0.179 ± 0.027
0.3	0.399 ± 0.007	0.375 ± 0.016	0.285 ± 0.002	0.262 ± 0.027
1.0	0.639 ± 0.008	0.569 ± 0.067	0.462 ± 0.003	0.404 ± 0.028
3.0	1.034 ± 0.012	0.972 ± 0.023	0.756 ± 0.003	0.619 ± 0.027

[a]The averages in the table do not include the tri-modal wet-season simulation. The maximum supersaturation values for the tri-modal simulations are as follows: 0.199, 0.325, 0.578, and 1.007 for updraft velocities of 0.1, 0.3, 1.0, and 3.0 m s^{-1}, respectively.

in droplet concentrations (Figure 5), even though the maximum parcel supersaturation decreased (Table 3). The largest increase in droplet number occurred for the dry season because of the order of magnitude increase in aerosol concentration. In spite of only a 40% increase in N from the wet season to the transition period, the cloud droplet concentration increased by at least a factor of two. The large mode diameter in the transition period size distribution allows for more particles to activate at lower supersaturations. This increase in droplet concentration also induces a significant reduction in maximum parcel supersaturation (Table 3). Small changes in parcel supersaturation while activating aerosol near the mode diameter (i.e., transition period) have a greater effect than activating aerosol at the shoulder of the distribution (i.e., dry season); hence the difference in trends with respect to updraft velocity in Figures 5 and 6.

During the initial stages of cloud development, water vapor transport to the growing droplets may not be sufficiently rapid for small particles near their critical size to activate. Consequently, they can re-evaporate and become interstitial aerosol particles, which exert a negligible effect on the cloud optical properties and precipitation processes. These simulations reveal that kinetic limitations are important regardless of updraft velocity and cloud height for all measured Amazonian CCN spectra. Such results are not unexpected since kinetic effects have been shown to be present for number concentrations greater than 100 cm^{-3} [*Nenes et al.*, 2001b]. We calculate asymptotic values for $\alpha(z)$, and the results are summarized in Table 4. Kinetic effects become more apparent as updraft velocity decreases (e.g., smaller water vapor flux) and droplet concentrations increase (e.g., dry season). The use of an equilibrium activation assumption could lead to an overprediction of cloud droplet number by 20 and 35% for low updraft velocities of 0.1 m s^{-1} during the wet and dry seasons, respectively (Table 4).

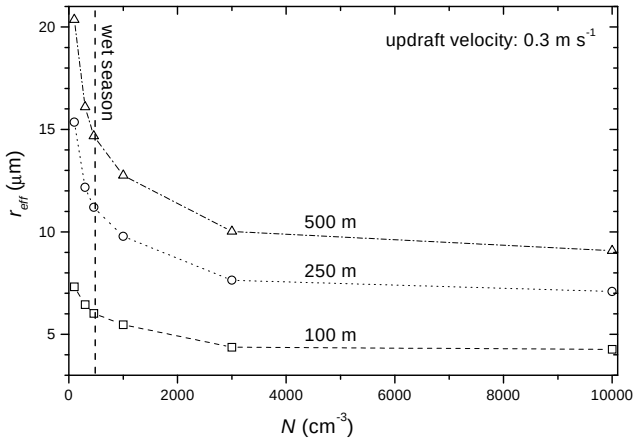

Figure 7. Predicted effective cloud radius as a function of increasing aerosol concentrations for a variety of cloud depths. The wet-season forest site CCN spectrum was used with an updraft velocity of 0.3 m s^{-1}. The cloud depth is indicated on each line.

6.2. Cloud Droplet Effective Radius

The higher aerosol number concentrations and larger mode diameters during the transition period and dry season reduce the effective radius by nearly a factor of two compared to the wet season (Figure 6). These results are not surprising given that the liquid water con-

Table 4. Simulated Asymptotic Alpha Ratios (N_{kn}/N_{th}) as a Function of Updraft Velocity Attained in the Cloud Parcel Model for Different Periods in the Amazon Basin.

	Maximum droplet ratio, $\alpha(z)$ (N_{kn}/N_{th})			
Updraft vel. (m s^{-1})	Wet season (forest)	Wet season (pasture)	Transition period	Dry season
0.1	0.800 ± 0.033	0.825 ± 0.019	0.765 ± 0.011	0.674 ± 0.033
0.3	0.869 ± 0.014	0.859 ± 0.008	0.853 ± 0.002	0.736 ± 0.019
1.0	0.890 ± 0.018	0.910 ± 0.023	0.913 ± 0.010	0.824 ± 0.017
3.0	0.936 ± 0.020	0.945 ± 0.007	0.958 ± 0.001	0.886 ± 0.010

tent is assumed to be the same. Indeed, it can be shown that for constant liquid water content, $r_{eff} \propto N_d^{-1/3}$ [*Twomey*, 1977]; an increase in N_d by a factor of 2.5 and 5.5 for the transition period and dry season result in ca. 30% and 45% reduction in effective cloud radii, respectively. A constant liquid water content and geometric standard deviation of the droplet distribution would merit a perfect $r_{eff} \sim N_d^{-1/3}$ dependence. However, even in a world of variations, this dependence still holds well [*Twomey*, 1977], given the narrow spread of droplet populations when growing via the diffusional mechanism. A more general relationship is: $r_{eff} \sim k^{-1/3} N_d^{-1/3}$, where $k = (r_v/r_{eff})^3$ and r_v is the volumetric average radius of the distribution [*Brenguier et al.*, 2000]. *In-situ* observations have shown that k varies from 0.67 in continental air masses to 0.80 in marine ones [*Martin et al.*, 1994], meaning that in these drastically different airmasses, $r_{eff} \sim 1.142 N_d^{-1/3}$ in the former and $r_{eff} \sim 1.077 N_d^{-1/3}$ in the latter.

As one would expect, the trends in r_{eff} with respect to updraft velocity reflect the N_d^{-3} dependence, which is reported in the previous section. These results are supported by satellite images taken over the Amazon Basin, which show that the presence of dense smoke can reduce the remotely sensed drop radius of continental cloud drops from 14 to 9 μm [*Kaufman and Fraser*, 1997].

Although collision and coalescence is not included in the simulation, the large reduction in r_{eff} reduces the probability for collision with other droplets [*Pruppacher and Klett*, 1997], and thus the chance of rain formation by liquid phase processes. Although the differences between the forest and pasture site CCN spectra lead to only modest changes in cloud properties, sensitivity of r_{eff} is greatest at low aerosol concentrations (Figure 7), such as those found during the wet season. Hence, a slight increase in N_d (Figure 5) due to anthropogenic sources could support AVHRR analysis, which shows a larger reduction in r_{eff} during the wet season compared to the dry season (T. Nakajima, personal communication, 2000). Other mechanisms, such as changes in direct and indirect forcing and subsequent effects on convection and clouds, are beyond the scope of this paper, but should also be investigated.

6.3. Cloud Albedo

A change in cloud albedo larger than ca. 0.005 can be considered climatically important; this albedo change can potentially exert a diurnally-averaged radiative forcing of nearly –1 W m^{-2} [*Eltahir and Humphries*, 1998]. Since we have used a 1-D model, the albedo and maximum albedo differences are a parameterization to measure the maximum aerosol effect within a cloud layer. Since we express everything in terms of maximum cloud albedo difference, cloud height becomes a free parameter in our calculations, and thus, can be interchanged with cloud thickness. The maximum aerosol effect on indirect radiative forcing has been estimated by comparing integrated cloud albedos for a given height of different simulations. Initially, the differences are small because the clouds are optically thin; whereas albedo converges to unity for optically thick non-absorbing clouds. Hence, albedo difference is a function of cloud depth and usually reaches a maximum within the first 300 m of the cloud. Figure 8 shows the maximum difference in cloud albedo for simulations using the measured Amazonian CCN spectra for non-absorbing clouds. The differences are positive due to the increasing droplet concentrations at the pasture site, and during the transition period and dry season. The wet-season forest site provides a reference for assessing the change in albedo.

The difference in cloud albedo between the forest and pasture site (Figure 8) does not appear to be signif-

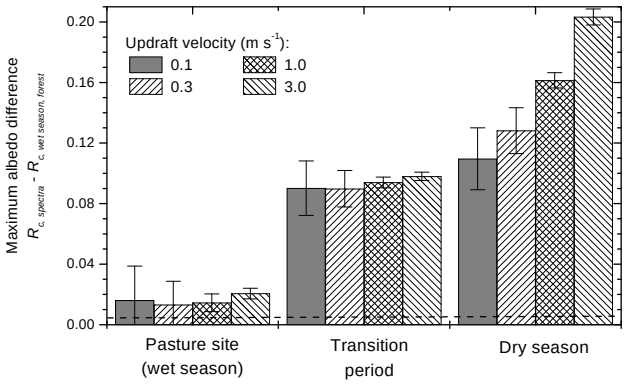

Figure 8. Predicted maximum albedo differences among measured CCN spectra in the Amazon Basin for different updraft velocities. The aerosol distributions in Table 1 are used and the wet-season forest case is used as a reference. The dashed lines represents a climatically significant radiative forcing of 1 W m^{-2} or a change in cloud albedo of 0.005.

icant because the number of activated droplets (Figure 3) is almost the same. This implies that during the wet season, the dominant driving force in climate change may result from the surface albedo change due to forest/pasture conversion. The surface albedo of the Amazon rain forest is between 0.11 and 0.13 [*Gash and Shuttleworth*, 1991]. Following deforestation, there will almost always be an increase in surface albedo. In Rondônia, the forest is often replaced by short grass for cattle grazing, which can result in surface albedos up to 0.25 [*Gash and Shuttleworth*, 1991]. Deforestation will thus result in a reduction in the amount of radiative energy that is absorbed by the earth's surface, resulting in less evaporation and a smaller driving force for convective activity [*Gash and Shuttleworth*, 1991]. A reduction in convective activity could inhibit precipitation; however, an inhomogeneous region of forest and pastures generates areas of local instability, which could actually increase the incidence of convective activity [*Baidya and Avissar*, 2002].

Significant enhancements in cloud albedo are calculated to result from the addition of smoke aerosol (Figure 8). The maximum change in albedo between the wet and dry seasons (assuming non-absorbing clouds) is 0.20, which corresponds to an inter-seasonal indirect aerosol forcing up to ca. –27 W m^{-2}. These simulated values for indirect forcing are comparable to the direct forcing from biomass-burning aerosol reported by *Ross et al.* [1998]. Albedo difference is primarily dependent on droplet concentration; hence, changes in albedo difference, shown in Figure 8, follow similar trends as droplet concentration (Figure 5). The results from our modeling studies represent the upper limit of the aerosol effect, since we did not include the effect of the absorption of incoming solar radiation due to the absorbing components of the smoke aerosol. A comparison of the AVHRR analysis and our modeling studies suggests that absorption of sunlight due to smoke aerosol may compensate for about half of the maximum aerosol effect shown in Figure 8.

The quantity used for assessing the importance of kinetic effects on cloud activation, in terms of cloud albedo, is the difference between thermodynamic and kinetic albedo. The discrepancy in albedo comes from the difference in simulated cloud droplet number concentration between the two approaches to predicting cloud droplet activation and growth. The thermodynamic albedo tends to be higher than the kinetic albedo, because the same amount of liquid cloud water is shared among a larger number of cloud droplets. The height at which the maximum difference occurs decreases with increasing updraft velocity and number concentration. The dry-season distribution exhibits the largest albedo difference, shown in Figure 9, due to enhanced kinetic effects. Wet season (i.e., pasture and forest sites) and transition period conditions result in comparable differences (Figure 9). The differences in albedo from kinetic effects, however, are small compared to the increase in albedo resulting from enhanced aerosol concentrations during biomass burning.

7. Effect of Aerosol Chemical Composition on Cloud Properties

Sensitivity tests using the wet- and dry-season CCN spectra have been performed to determine the influence of the physical and chemical characteristics of an aerosol population on CCN activity and their subsequent growth into cloud droplets. Variations in CCN populations change the maximum in-cloud supersaturation, because particles that activate into cloud droplets at low supersaturations effectively scavenge the available water vapor. Therefore the CCN spectra that extend into lower supersaturations (i.e., WM and DDST; Figure 2) exhibit the lowest attained in-cloud supersaturations compared to other simulations of the respective season. WC and DC, whose CCN spectra are shifted to higher supersaturations, exhibit the highest in-cloud supersaturations, implying that surface-tension effects

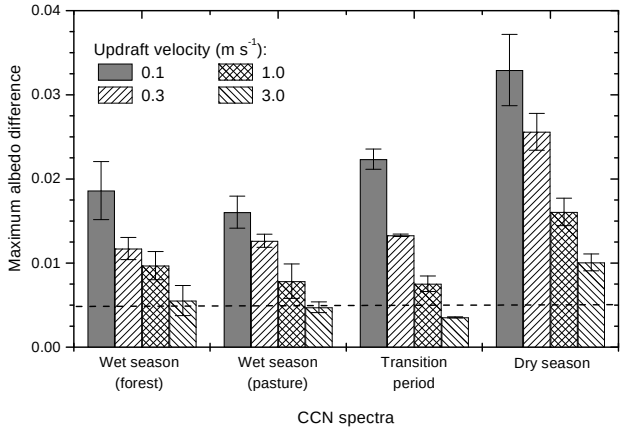

Figure 9. Maximum differences between thermodynamically and kinetically predicted cloud albedo for different updraft velocities. The aerosol distributions in Table 1 are used. The dashed lines represents a climatically significant radiative forcing of 1 W m^{-2} or a change in cloud albedo of 0.005.

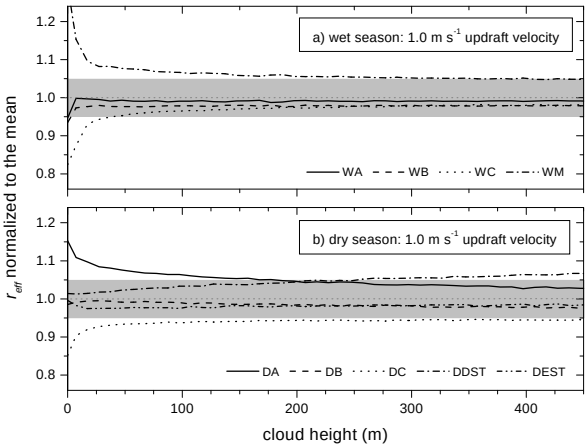

Figure 10. Effective radius for each distribution normalized to the mean. Wet- and dry-season profiles from Table 1 are shown for an updraft velocity of 1.0 m s^{-1}. The shaded area indicates the region of reff within 5% of the mean. The simulations (WA, WB, etc.) are defined in Table 1.

and the presence of GCCN could play an important role in droplet growth.

Because of the nonlinear feedback of the changing aerosol growth histories (from changes in chemical composition) into supersaturation profiles, the effect of chemistry on cloud droplet number, effective radius, and cloud albedo is not intuitive. We will take a closer look at the differences between the wet- and dry-season spectra in the following sections.

7.1. Wet-season CCN Spectra

CCN spectra resulting from the modeled size distributions presented in Table 1 closely resemble the measured wet-season spectra between 0.15 and 1.5 % S_v (Figure 2a). Activation and growth of the cloud droplets were similar between the single mode distributions in spite of the differences in assumed chemical composition, as shown in Figure 10a. Hence, differences in cloud albedo are suspected to be less influenced by aerosol chemistry during the wet season. The larger effective radius resulting from the tri-modal distribution, however, can have a significant impact on indirect radiative forcing. For example, *Ghan et al.* [2001] found that a decrease in global mean cloud effective radius by 4.3% exerted an indirect forcing of nearly -1 W m^{-2}.

The tri-modal distribution exhibited larger droplets due to the activation of the 0.90 μm mode. This large mode is a source of GCCN, which could be important for initiating precipitation processes [*Yin et al.*, 2000]. Although collision and coalescence were not included in the simulation, strong kinetic effects may enhance the precipitation process, because the driving force for droplet growth (i.e., the difference between the saturation ratio at the droplet surface and that of the surrounding air) is greater for larger droplets. Hence larger droplets, which are necessary to initiate collision and coalescence, could effectively draw water vapor away from the smaller droplets. The competition for water vapor by GCCN will likely be enhanced at higher aerosol concentrations when kinetic limitations are more pronounced. A strong kinetic effect, however, could also decrease the precipitation efficiency because the overall droplet population becomes smaller due to evaporative and deactivation mechanisms shown in *Nenes et al.* [2001b]. This question should be addressed in future studies.

7.2. Dry-season CCN Spectra

In spite of the similarity of the modeled dry-season CCN spectra to the measured results between 0.15 and 1.5% S_v (Figure 2b), variations in number distribution and chemical composition can yield climatically significant differences in cloud properties. The non-converging behavior of the effective cloud radii for the dry-season simulations, shown in Figure 10b, illustrates the differences in activation and growth of the cloud

droplets. Relative differences in cloud effective radius between simulations can exceed 10%, which could yield differences in indirect forcing as high as 2 W m^{-2} [*Rotstayn*, 1999]. These results suggest that changes in cloud albedo are more influenced by chemical and physical properties in cases of high aerosol concentrations, such as those found during the biomass-burning season.

The importance of chemical composition and the influence of kinetic effects for the dry-season CCN spectra are highlighted by DDST and DEST (Table 1; Figure 10b), where the slower initial rate of droplet activation allows a few particles to grow into cloud droplets before kinetic limitations become significant at larger droplet concentrations. The enhanced CCN activity of larger particles (i.e., smaller critical supersaturation; Figure 2b) due to surface tension effects of DDST appears to effectively compete for water vapor as r_{eff} continues to increase relative to the mean droplet size. The surface tension effect essentially serves the same role as GCCN, and the kinetic limitations at high droplet concentrations appear to amplify this effect.

Although the CCN spectra of DA and DEST are nearly identical, even at smaller supersaturations than measured, Figure 10b illustrates significant differences in the activation and growth of the droplets. The difference in cloud effective radii for the two simulations is ca. 4.5%, which is of climatic significance [*Ghan et al.*, 2001], and could be related to surface tension effects. Surface tension effects not only reduce the droplet's critical supersaturation, but also influence the shape of the Köhler curve, which can alter the growth behavior of a droplet. Therefore, knowledge of the CCN spectra alone may not be adequate in fully assessing the climatic effects of aerosol.

8. Conclusions

We have investigated the change in cloud properties based on measured CCN spectra between 0.15 and 1.5% S_v during the wet and dry seasons in the Amazon Basin. CCN concentrations rise by nearly an order of magnitude from wet to dry seasons, which increase droplet concentrations up to a factor of seven at high updraft velocities. Throughout the text, we have compared the changes in cloud properties relative to wet-season forest CCN spectra. Although the differences between the forest and pasture site CCN spectra lead to only modest changes in cloud properties, the resulting modifications in cloud properties are most sensitive at low number concentrations, such as those that are found in wet-season conditions.

Our results indicate that knowledge of the CCN spectra alone is insufficient to fully capture the climatic influence of biomass burning. The activation and growth behavior of CCN are shown to be influenced by subtle variations in the size distribution and chemical composition, which are not well constrained by our measurements. Kinetic limitations to droplet activation and growth reduce droplet concentrations by up to 20% in the wet season and 35% in the dry season as compared with simulations based on equilibrium Köhler theory. Kinetic effects are, however, small compared to the predicted changes in cloud properties induced by biomass-burning aerosol.

Human activity, such as industrial emissions and biomass burning, modifies physical and chemical properties of the aerosol population – components that dictate CCN activity – and could lead to important changes in cloud properties that govern the energy and water cycle within the Amazon Basin. The response of cloud droplet concentration to changes in CCN concentrations is the basis for the modification of precipitation, cloud fraction, and indirect forcing. However, changes in surface albedo have not been included in this study and are an important driving force in the hydrological cycle and convective activity. Light-absorbing substances in smoke darken the Amazonian clouds, and our modeling studies suggests that absorption of sunlight due to smoke aerosol may compensate for about half of the maximum aerosol effect. An increase in aerosol concentrations during the wet season will likely have a greater effect on the rain forest climate than further intensification of biomass burning during the dry season, due to the higher sensitivity at the low ambient aerosol concentrations.

Acknowledgments. We thank G. Lala and P. Guyon for support with building the CCN instruments. These experiments would not be possible without support from the following Brazilian institutions: INPE, CPTEC, IBAMA, INCRA, and UNIR. This project was supported by the Max Planck Gesellschaft and by the European Commission (Project EUSTACH-LBA). G.R. was funded by the Max Planck Institute for Chemistry and by Environment Now at the California Institute of Technology. This work was also supported by Office of Naval Research grant N00014-96-0119.

References

Albrecht, B., Aerosols, cloud microphysics, and fractional cloudiness, *Science*, *245*, 1227–1230, 1989.

Andreae, M., Biogeochemical cycling of carbon, water, energy, trace gases and aerosols in Amazonia: The LBA-

EUSTACH experiments, *Geophys. Res. Lett.*, *in press*, 2002.

Baidya, R., and R. Avissar, Impact of land use/land cover change on regional hydrometeorology in the Amazon., *J. Geophys. Res.*, *submitted*, 2002.

Brenguier, J., Y. Fouquart, and L. Schüller, Radiative properties of boundary layer clouds: Optical thickness and effective radius versus geometrical thickness and droplet concentration., *J. Aerosol Sci.*, *57*, 803–821, 2000.

Eltahir, E., and E. Humphries, The role of clouds in the surface energy balance over the Amazon forest., *Int. J. Climatol.*, *18*, 1575–1591, 1998.

Facchini, M., M. Mircea, S. Fuzzi, and R. Charlson, Cloud albedo enhancement by surface-active organic solutes in growing droplets, *Nature*, *401*, 257–259, 1999.

Fuzzi, S., S. Decesari, M. Facchini, E. Matta, and M. Mircea, A simplified model of the water soluble organic component of atmospheric aerosols., *Geophys. Res. Lett.*, *20*, 4079–4082, 2001.

Gash, J., and W. Shuttleworth, Tropical deforestation:Albedo and the surface-energy balance., *Climatic Change*, *19*, 123–133, 1991.

Ghan, S., R. Easter, E. Chapman, H. Abdul-Razzak, Y. Zhang, L. Leung, N. Laulainen, R. Saylor, and R. Zaveri, A physically based estimate of radiative forcing by anthropogenic sulfate aerosol., *J. Geophys. Res.*, *106*, 5279–5293, 2001.

Hobbs, P., D. Bowdle, and L. Radke, Particles in the lower troposphere over the high plains of the United States, 2. Cloud condensation nuclei., *J. Clim. Meteorol.*, *24*, 1358–1369, 1985.

Hudson, J., and A. Clarke, Aerosol and cloud condensation nuclei measurements in the Kuwait plume., *J. Geophys. Res.*, *97*, 14,533–14,536, 1992.

Hudson, J., and P. Frisbie, Surface cloud condensation nuclei and condensation nuclei measurements at Reno, Nevada., *Atmos. Environ.*, *25*, 2285–2299, 1991.

Kaufman, Y., and R. Fraser, The effect of smoke particles on clouds and climate forcing., *Science*, *277*, 1636–1639, 1997.

Kaufman, Y., and T. Nakajima, Effect of Amazon smoke on cloud microphysics and albedo - Analysis from satellite imagery., *J. Appl. Meteorol.*, *32*, 729–744, 1993.

Kaufman, Y., A. Setzer, D. Ward, D. Tanré, B. Holben, P. Menzel, M. Pereira, and R. Rasmussen, Biomass burning airborne and spaceborne experiment in the Amazonas (BASE-A)., *J. Geophys. Res.*, *97*, 14,581–14,599, 1992.

Kaufman, Y., P. Hobbs, V. Kirchhoff, P. Artaxo, M. King, and D. Ward, Smoke, Clouds, and Radiation - Brazil (SCAR-B) experiment., *J. Geophys. Res.*, *S*, 1998.

Kleeman, M., J. Schauer, and G. Cass, Size and composition distribution of fine particulate matter emitted from motor vehicles., *Environ. Sci. Technol.*, *34*, 1132–1142, 2000.

Lacis, A. A., and J. E. Hansen, A parameterization for the absorption of solar radiation in the earth's atmosphere, *J. Aerosol Sci.*, *31*, 118–133, 1974.

Lala, G., and J. Jiusto, An automatic light scattering CCN counter, *J. Appl. Meteorol.*, *16*, 413–418, 1977.

Lide, D., *CRC Handbook of Chemistry and Physics*, CRC Press, Cleveland, Ohio, 2000.

Martin, G., D. Johnson, and A. Spice, The measurement and parameterization of effective radius of droplets in warm stratocumulus clouds., *J. Aerosol Sci.*, *51*, 1823–1842, 1994.

Mason, B., *Principles of Geochemistry*, John Wiley, New York, 1966.

Mayol-Bracero, O., P. Guyon, B. Graham, G. Roberts, M. Andreae, S. Decesari, M. Facchini, S. Fuzzi, and P. Artaxo, Water-soluble organic compounds in biomass burning aerosols over Amazonia: 2. Apportionment of the chemical composition and importance of the polyacidic fraction., *J. Geophys. Res.*, *LBA Special Issue, in press*, 2002.

Nenes, A., P. Chuang, R. Flagan, and J. Seinfeld, A theoretical analysis of cloud condensation nucleus (CCN) instruments, *J. Geophys. Res.*, *106*, 3449–3474, 2001a.

Nenes, A., S. Ghan, H. Abdul-Razzak, P. Chuang, and J. Seinfeld, Kinetic limitations on cloud droplet formation and impact on cloud albedo, *Tellus B*, *53*, 133–149, 2001b.

NOAA-ARL, HYSPLIT 4, hybrid single-particle lagrangian integrated trajectory model, *Tech.rep.*, NOAA Air Resources Laboratory, Silver Spring, MD., 1997.

Pruppacher, H., and J. Klett, *Microphysics of Clouds and Precipitation*, 2nd ed., Kluwer, Dordrecht, 1997.

Reid, J., P. Hobbs, R. Ferek, D. Blake, J. Martins, M. Dunlap, and C. Liousse, Physical, chemical, and optical properties of regional hazes dominated by smoke in Brazil., *J. Geophys. Res.*, *103*, 32,059–32,080, 1998.

Roberts, G., Cloud condensation nuclei in the amazon basin: Their role in a tropical rainforest, Ph.D. thesis, California Institute of Technology, Pasadena, CA, 2001.

Roberts, G., J. Zhou, P. Artaxo, and M. Andreae, Cloud condensation nuclei in the Amazon Basin: "Marine" conditions over a continent?, *Geophys. Res. Lett.*, *28*, 2807–2810, 2001a.

Roberts, G., J. Zhou, E. Swietlicki, P. Artaxo, and M. Andreae, Sensitivity of CCN spectra on chemical and physical properties of aerosol., *Geophys. Res. Lett.*, *28*, 2807–2810, 2001b.

Rosenfeld, D., TRMM observed first direct evidence of smoke from forest fires inhibiting rainfall., *Geophys. Res. Lett.*, *26*, 3105–3108, 1999.

Ross, J., P. Hobbs, and B. Holben, Radiative characteristics of regional hazes dominated by smoke from biomass burning in Brazil: Closure tests and direct radiative forcing., *J. Geophys. Res.*, *103*, 31,925–31,941, 1998.

Rotstayn, L., Indirect forcing by anthropogenic aerosols: A global climate model calculation of the effective-radius and cloud-lifetime effects., *J. Geophys. Res.*, *104*, 9369–9380, 1999.

Seinfeld, J., and S. Pandis, *Atmospheric chemistry and physics: from air pollution to climate change*, John Wiley, New York, 1998.

Setzer, A., and M. Pereira, Amazon biomass burnings in 1987 and their tropospheric emissions., *Ambio*, *20*, 19–22, 1991.

Twomey, S., The influence of pollution on the shortwave albedo of clouds, *J. Aerosol Sci.*, *34*, 1149–1152, 1977.

Williams, E. *et al.*., Observational tests of the aerosol hypothesis for precipitation and electrification in Rondonia, Brazil., *J. Geophys. Res.*, *LBA Special Issue, in press*, 2002.

Yin, Y., Z. Levin, T. Reisin, and S. Tzivion, The effects of giant cloud condensation nuclei on the development of precipitation in convective clouds - a numerical study., *Atmos. Res.*, *53*, 91–116, 2000.

Zhou, J., E. Swietlicki, H. Hansson, and P. Artaxo, Submicrometer aerosol particle size distribution and hygroscopic growth measurements in the Amazonian rain forest during the wet season., *J. Geophys. Res.*, *LBA Special Issue, in press*, 2002.

G. Roberts, Scripps Institution of Oceanography, Center for Atmospheric Research, University of California, San Diego, CA 92093. (e-mail: greg@borneo.ucsd.edu)

A. Nenes and J. H. Seinfeld, Department of Chemical Engineering, California Institute of Technology, Pasadena, CA, 91125. (e-mail: nenes@caltech.edu; seinfeld@caltech.edu)

M. Andreae, Max Planck Institute for Chemistry, Biogeochemistry Dept., P.O. Box 3060, D-55020 Mainz, Germany (e-mail: moa@mpch-mainz.mpg.de)

Received June 19, 2001; revised February 26, 2002; accepted March 30, 2002.